Superfluidity and Coherence in Bose-Einstein Condensates

Wolfgang Ketterle
Research Laboratory for Electronics, MIT-Harvard Center for Ultracold Atoms, and Department of Physics
Massachusetts Institute of Technology, Cambridge, MA 02139, USA
e-mail: ketterle@mit.edu

This paper summarizes recent work at MIT which was presented at the Nobel Jubilee Symposium. These examples demonstrate the broad range of topics which are covered by research on quantum-degenerate gases: superfluidity, phonons, boson and fermion mixtures, atom optics. For further reading and references to other work, we refer to the original publications.

PACS numbers: 03.75.Fi, 05.30.Fk, 32.80.Pj, 39.10.+j, 39.25. +k, 67.40.Vs, 67.60.-g

1. Observation of Vortex Lattices in Bose-Einstein Condensates

Quantized vortices play a key role in superfluidity and superconductivity. In superconductors, magnetic flux lines arrange themselves in regular lattices that have been directly imaged. In superfluids, direct observation of vortices had been limited to small arrays (up to 11 vortices), both in liquid ^{4}He [1] and more recently in rotating gaseous Bose-Einstein condensates (BEC) [2, 3].

We have observed the formation of highly-ordered vortex lattices in a rotating Bose-condensed gas [4]. They were produced by rotating the condensate around its long axis using the optical dipole force exerted by a blue-detuned laser. A striking feature of the observed lattices is the extreme regularity, free of any major distortions, even near the boundary. Such "Abrikosov" lattices were first predicted for quantized magnetic flux lines in type-II superconductors. The observed triangular lattices contained over 100 vortices with lifetimes of several seconds (Figure 1). Individual vortices persisted up to 40 s. The lattices could be generated over a wide range of rotation frequencies and trap geometries, shedding light on the formation process. Our observation of lattice dislocations, irregular structure and dynamics indicate that gaseous Bose-Einstein condensates may be a model system for the study of vortex matter.

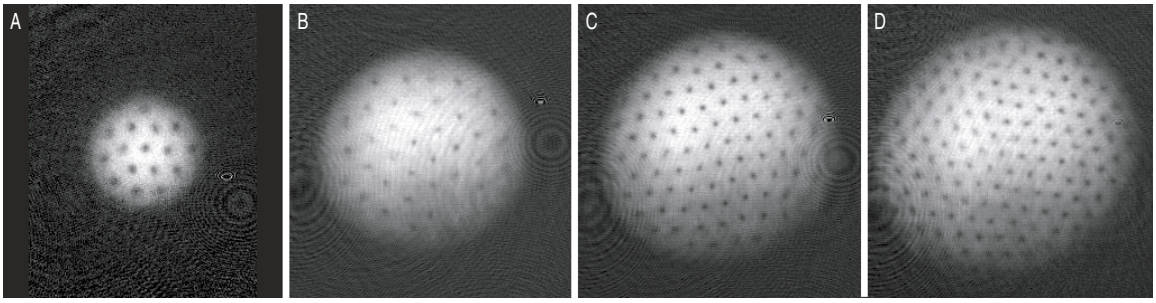

Figure 1: Observation of vortex lattices [4]. The examples shown contain (A) 16 (B) 32 (C) 80 and (D) 130 vortices. The vortices have "crystallized" in a triangular pattern. The diameter of the cloud in (D) was 1 mm after ballistic expansion which represents a magnification of 20.

2. Vortex Nucleation in a Stirred Bose-Einstein Condensate

Dissipation and turbulence in superfluid flow often involves the creation and subsequent motion of quantized vortices. Since vortices are topological defects they may only be created in pairs, or can enter a system individually from its boundary. The nucleation process has been a subject of much theoretical interest [5]. Experiments with Bose-Einstein condensates in atom traps are well suited to test theories of nucleation because the boundary of the condensate is well controlled, and vortices can be directly imaged.

In previous work, we had observed vortex lattices in stirred Bose-Einstein condensates [4]. By varying the stirring parameters we explored different mechanisms for vortex nucleation [6]. A large stirrer, with a beam waist comparable to the condensate radius showed enhanced vortex generation at discrete frequencies. Figure 2 shows the number of vortices versus the frequency of rotation of the laser beam using 2-, 3- and 4-point patterns for the stirring beams. These resonances were close to the frequencies of excitation for surface modes of different multipolarity. This observation confirms the role of discrete surface modes in vortex formation.

However, when we used a tightly focused (beam waist 5 μm) laser beam as stirrer, we observed a broad response as a function of the frequency of the stirrer's motion, and no resonances (see Figure 2). Furthermore, vortices could be generated well below the critical rotation frequency for the excitation of surface modes. This suggests a local mechanism of vortex generation involving hydrodynamic flow and local turbulence.

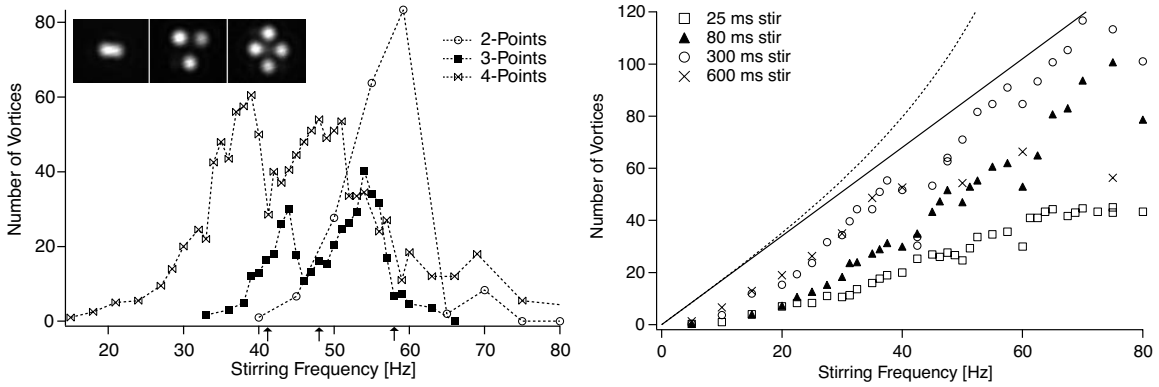

Figure 2: Discrete resonances in vortex nucleation (left) [6]. The number of vortices created by multi-point patterns is shown. The arrows below the graph show the positions of the surface mode resonances. The stirring times were 100 ms for the 2- and 3-point data, and 300 ms for the 4-point data. Inset shows 2-,3-, and 4-point dipole potentials produced by a 25 μm waist laser beam imaged onto the CCD camera.
Non-resonant nucleation using a small stirrer (right). Average number of vortices created for different stirring times using a 2-point pattern positioned at the edge of the condensate.

3. Observation of vortex phase singularities in Bose-Einstein condensates

Bose-Einstein condensates of dilute atomic gases offer a unique opportunity to study quantum hydrodynamics. The low density of the gas allows direct comparison with first principle theories.

Recently, vortices in a Bose-Einstein condensate have been realized experimentally and are currently under intensive study [3, 4, 7]. In most of this work, vortices were identified by observing the density depletion at the cores. The velocity field was inferred only indirectly, with the exception of the work on circulation in a two-component condensate [7]. The flow field of a vortex can be directly observed when the phase of the macroscopic wavefunction is measured using interferometric techniques. In our work, we created one or several vortices in one condensate by moving a laser beam through it and imaged its phase by interfering it with a second unperturbed condensate which served as a local oscillator [8].

The characteristic signature of vortices were dislocations in the interference fringes. The "extra" fringe which terminates at the vortex core corresponds to one quantum of circulation h/m (where m is the atomic mass and h Planck's constant) or a phase change of 2π integrated along a path around the vortex core (Figure 3).

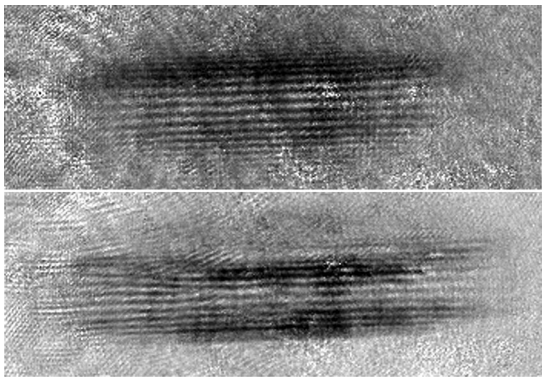

Figure 3: Observation of the phase singularities of vortices created by sweeping a laser beam through a condensate [8]. Without the sweep, straight fringes of about 20 μm spacings were observed (upper image), while after the sweep, fork-like dislocations appeared (lower image). The speed of the sweep was 1.1 μm/ms corresponding to a Mach number of 0.1. The field of view of each image is 1.1 mm x 0.38 mm.

4. Two species mixture of quantum degenerate Bose and Fermi gases

Experimental methods of laser and evaporative cooling, used in the production of atomic Bose-Einstein condensates have recently been extended to realize quantum degeneracy in trapped Fermi gases [9]. Fermi gases are a new rich system to explore the implications of Pauli exclusion on scattering properties of the system, and ultimately fermionic superfluidity.

We have produced a new macroscopic quantum system, in which a degenerate ^{6}Li Fermi gas coexists with a large and stable ^{23}Na BEC [10]. This was accomplished using inter-species sympathetic cooling of fermionic ^{6}Li in a thermal bath of bosonic ^{23}Na. We have achieved high numbers of both fermions ($>10^5$) and bosons ($>10^6$), and ^{6}Li quantum degeneracy corresponding to one half of the Fermi temperature (Figure 4). This is the first time that a Fermi sea was produced with a condensate as a "refrigerator".

Low rates for both intra- and inter-species inelastic collisions result in a lifetime longer than 10 s. Hence, in addition to being the starting point for studies of the degenerate Fermi gas, this system shows great promise for studies of degenerate Bose-Fermi

mixtures, including collisions between the two species, and of limitations to the sympathetic cooling process.

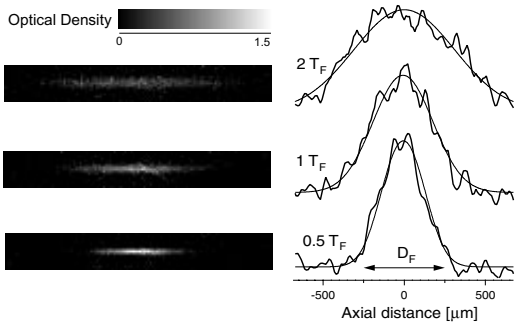

Figure 4: Onset of Fermi degeneracy [10]. Three pairs of images (top to bottom) correspond to T/T_F= 2, 1, and 0.5. (a) Column densities of the ^{6}Li cloud were recorded by absorption imaging. (b) Axial line density profiles and the Fermi-Dirac fits to the data are plotted. The arrow indicates the size of the Fermi diameter, D_F, which is the diameter of the cloud at zero Kelvin.

5. *Experimental observation of the Bogoliubov transformation for a Bose-Einstein condensed gas*

The pioneering paper by Bogoliubov in 1947 was the starting point for a microscopic theory of superfluidity [11]. Bogoliubov found the non-perturbative solution for a weakly interacting gas of bosons. The main step in the diagonalization of the Hamiltonian is the famous Bogoliubov transformation, which expresses the elementary excitations (or quasi-particles) with momentum q in terms of the free particle states with momentum +q and –q. For small momenta, the quasiparticles are a superposition of +q and -q momentum states of free particles.

Following the theoretical suggestion in ref. [12] we observed such superposition states by first optically imprinting phonons with wavevector q into a Bose-Einstein condensate and probing their momentum distribution using Bragg spectroscopy with a high momentum transfer (Figure 5). By combining both momentum and frequency selectivity, we were able to "directly photograph" the Bogoliubov transformation [13].

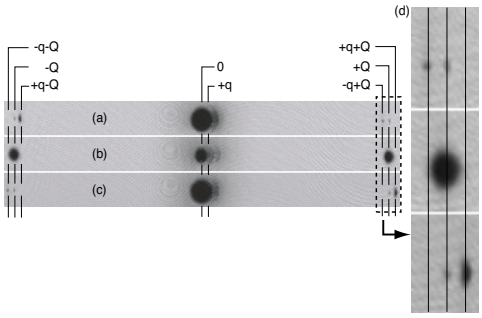

Figure 5: Momentum distribution of a condensate with phonons [13]. After imprinting +q phonons into the condensate, momentum analysis via Bragg spectroscopy transfers a momentum ±Q (two photon recoil) to the atoms. Absorption images after 40 ms time of flight in (a), (b), and (c) show the condensate in the center and outcoupled atoms to the right and left for probe frequencies of 94, 100, and 107 kHz, respectively. The small clouds to the right of the condensate are phonons which were converted to free

particles. The size of the images is 25 x 2.2 mm. (d) The outlined region in (a) - (c) on the right is magnified, and clearly shows outcoupled atoms with momenta Q±q, implying that phonons with wavevector q/$\hbar$ have both +q and -q free particle momentum components.

6. Transport of Bose-Einstein Condensates with Optical Tweezers

Conventional condensate production techniques severely limit optical and mechanical access to experiments due to the many laser beams and magnetic coils needed to create BECs. This conflict between cooling infrastructure and accessibility to manipulate and study condensates has been a major restriction to previous experiments. So far, most experiments were carried out within a few millimeters of where the condensate was created. What is highly desirable is a condensate "beam line" that delivers condensates to a variety of experimental platforms.

We have transported gaseous Bose-Einstein condensates over distances up to 44 cm [14]. This was accomplished by trapping the condensate in the focus of an infrared laser and translating the location of the laser focus with controlled acceleration. Condensates of order 10^6 atoms were moved into an auxiliary "science" chamber which has excellent optical and mechanical access. This technique is ideally suited to deliver condensates close to surfaces, e.g., to microscopic waveguides and into electromagnetic cavities. As a proof-of-principle demonstration, we have used the tweezers technique to transfer condensates into a magnetic trap formed by a Z-shaped wire suspended in the science chamber (Figure 6). The same procedure can now be used to load condensates into atom chips In such devices, patterns of wires are lithographically deposited on a surface and may allow the realization of single-mode waveguides and atom interferometers.

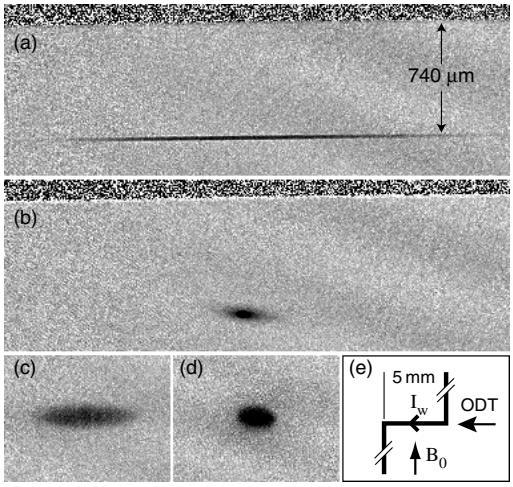

Figure 6: Absorption images of condensates in the science chamber, side view [14]. All images have the same scale. Condensates of ≈ 6 10^5 atoms are shown in (a) optical trap and (b) wire-trap. The center segment of the Z-shaped wire is visible as a dark speckled horizontal strip and is 740 µm above the trapped atoms. The condensate was released from (c) an optical trap and observed after 10 msec time of flight and (d) from a wiretrap after 23 ms time of flight. (e) Schematic of the wiretrap, top view. I_w = 2 A is the current through the wire, and B_0= 2.9 G is the bias field. Atoms are trapped below the 5-mm-long central segment of the wire, which is aligned with the optical trap axis. The wiretrap was located 36 cm from where the condensates were produced.

1. E.J. Yarmchuk, M.J.V. Gordon, and R.E. Packard, Phys. Rev. Lett. **43**, 214 (1979).
2. K.W. Madison, F. Chevy, W. Wohlleben, and J. Dalibard, J. Mod. Opt. **47**, 2715 (2000).
3. K.W. Madison, F. Chevy, W. Wohlleben, and J. Dalibard, Phys. Rev. Lett. **84**, 806 (2000).
4. J.R. Abo-Shaeer, C. Raman, J.M. Vogels, and W. Ketterle, Science **292**, 476 (2001).
5. A.L. Fetter and A.A. Svidzinsky, J. Phys.: Condens. Matter **13**, R135 (2001).
6. C. Raman, J.R. Abo-Shaeer, J.M. Vogels, K. Xu, and W. Ketterle, Phys. Rev. Lett. **87**, 210402 (2001).
7. M.R. Matthews, B.P. Anderson, P.C. Haljan, D.S. Hall, C.E. Wieman, and E.A. Cornell, Phys. Rev. Lett. **83**, 2498 (1999).
8. S. Inouye, S. Gupta, T. Rosenband, A.P. Chikkatur, A. Görlitz, T.L. Gustavson, A.E. Leanhardt, D.E. Pritchard, and W. Ketterle, Phys. Rev. Lett. **87**, 080402 (2001).
9. B. DeMarco and D.S. Jin, Science **285**, 1703 (1999).
10. Z. Hadzibabic, C.A. Stan, K. Dieckmann, S. Gupta, M.W. Zwierlein, A. Görlitz, and W. Ketterle, preprint cond-mat/0112425.
11. N.N. Bogoliubov, J. Phys. (USSR) **11**, 23 (1947).
12. A. Brunello, F. Dalfovo, L. Pitaevskii, and S. Stringari, Phys. Rev. Lett. **85**, 4422 (2000).
13. J.M. Vogels, K. Xu, C. Raman, J.R. Abo-Shaeer, and W. Ketterle, preprint cond-mat/0109205.
14. T.L. Gustavson, A.P. Chikkatur, A.E. Leanhardt, A. Görlitz, S. Gupta, D.E. Pritchard, and W. Ketterle, Phys. Rev. Lett. **88**, 020401 (2002).